As originally published in the SMTA Proceedings.

Experimental Investigation of Solid-State Diffusion between Rolled Cu and Electroplated Matte-Sn System

Abhilaash Ajith Kumar, Werner Hügel, Ph.D.
Robert Bosch GmbH
Schwieberdingen, Germany
Abhilaash.Ajithkumar@de.bosch.com

ABSTRACT

Ever increasing need for miniaturization and high-density electronics, leads to higher intermetallic (IMC) phase/solder ratio affecting the ductility of the solder joint. The diffusion behavior and growth of intermetallic (IMC) phases of Cu-Sn system is studied through isothermal aging over wide range of temperature from 398K to 473K. Cu-Sn binary couples, prepared by electroplating Sn over bulk Cu, are aged at 398K, 423K, 453K and 473K for various times to investigate the microstructural development and growth kinetics of the IMC phases. In-house developed algorithm was used to detect and quantify the Cu_6Sn_5 and Cu_3Sn morphology from electron microscopy images. Considering the narrow compositional range and interdependent growth/dissolution of the two IMC phases, Wagner's method is used to evaluate the integrated interdiffusion coefficients based on the measured IMC thicknesses. The activation energies and the diffusion constants of the Cu_6Sn_5 and Cu_3Sn IMC phases have been calculated from the integrated interdiffusion coefficients.

Key words: Activation Energy, Cu-Sn, Diffusion, Intermetallics, Isothermal Aging

INTRODUCTION

Need for high density electronics and high temperature service requirements for power electronics in electric automobiles in recent years, have reduced solder joint dimensions and increased the temperature requirements of reliability upto 473K. With such requirements, the intermetallic (IMC) phases that form at the interface between the metal substrate and the solder influence the reliability performance of the solder joint. Nearly 80% of all electronic components use rolled Cu plates as the lead-frame material and the interfacial reactions that lead to the formation of Cu_6Sn_5 and Cu_3Sn IMC phases are important to understand to design the automotive electronic components. Several studies involving pure Cu-Sn bulk system have been conducted to study the interdiffusion reactions and estimate the growth rate of the two IMC phases [1]–[4]. The growth rates reported are applicable to only bulk Cu-Sn binary couples which are rarely encountered in automotive electronic components. Moreover, the diffusion coefficients and the activation energies reported in these studies have large discrepancies due to different experimental conditions and not applicable to industrial service conditions.

This study focusses on the IMC phase growth in rolled Cu-electroplated Sn system during the temperature range from 398K to 473K. Inhouse developed image segmentation program detects and quantifies the IMC phases from the electron microscopy images. In addition, the integrated interdiffusion coefficients and the activation energies Cu_6Sn_5 and Cu_3Sn have been calculated.

EXPERIMENTAL

Pure Cu rolled plates were electroplated with matte-Sn (average Sn grain size 3-5 µm) thickness of 20±2 µm under standard industrial conditions. The matte-Sn electroplated plates were cut into 5 mm x 5 mm samples and were placed in a temperature-controlled convection oven under ambient conditions at the respective temperatures for specified times as seen in table 1. The temperature calibration was done using a K-type thermocouple (±2K). Once the isothermal aging is complete, the samples were immediately quenched in cold water to stop the diffusion process.

The aged samples were epoxy cold mounted (for 8 hours atleast) and subjected to grinding and polishing to obtain a polished surface of the cross section containing Cu, IMC and Sn. A final colloidal silica polish was done to all samples which slightly etches the polished surface and provides enhanced contrast between the different phases during subsequent electron microscopy.

Scanning electron microscopy (SEM) in the backscattered electron mode (BSE) was done after coating the polished surface with 5 nm Au via PVD process. The BSE mode further enhances the contrast between the different phases in the cross-section images because of its sensitivity to atomic mass. Energy dispersive spectroscopy (EDS) allowed composition measurement of the phases through point scans and line scans. The EDS equipment was calibrated to have error of ±0.5 at.%.

Table 1: Temperature aging conditions

Aging T (K)	Aging time (days)						
398	1	3	5	7	10	14	21
423	1	3	5	7	10	14	
453	1	3	5	7	10	14	
473	1	3	5	7	10	14	

The cross-section images from the SEM were analyzed through an in-house developed algorithm that automatically segmented the different IMC phases from the SEM image as seen in figure 1. The thicknesses of IMCs were measured at

each pixel width across the entire segmented image and a mean IMC thickness value has been calculated for every image. Mean values were calculated for minimum of 5 upto 10 images depending on the complexity of IMC morphology.

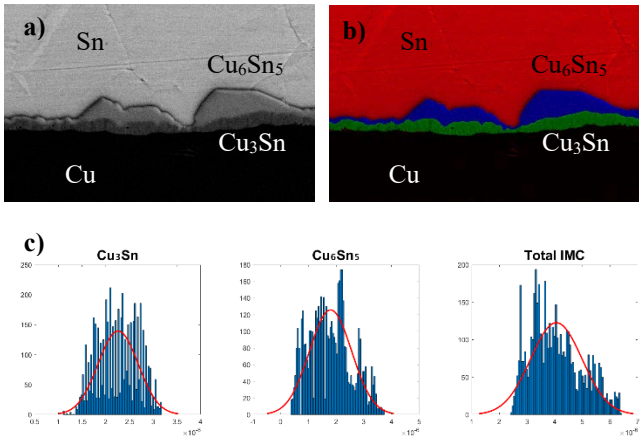

Figure 1: a) SEM cross-section image showing Cu, Cu_3Sn, Cu_6Sn_5 and Sn phases; b) Various phases detected from the image segmentation program; c) Histogram of the individual and total IMC thickness measured along each pixel column and normal fitting to find the mean and standard deviation.

Since two IMC phases of different compositions and narrow homogeneity range grow in the Cu-Sn diffusion system, it is essential to calculate the integrated interdiffusion coefficients (D_{int}) of the individual IMCs using Wagner method [5]. From the D_{int} values at various temperatures, the Arrhenius plot is used to calculate the diffusion constants (D_0) and the activation energies (E_a) for the individual IMC phases.

RESULTS AND DISCUSSION

IMC Microstructure

Figure 2 shows the back-scattered electron microscopy images of the cross-section of the Cu-Sn samples which were aged at 398K, 423K, 453K and 473K for 14 days. The two IMC phases Cu_3Sn and Cu_6Sn_5 can be clearly seen in all the temperatures. The morphology of the Cu_6Sn_5 is rough at the lower temperatures of 398K and 423K while at higher temperatures of 453K and 473K, it transitions towards a flatter morphology. In contrast, the morphology of the Cu_3Sn remains wavy throughout all temperatures and times.

As the IMC layer grows and thickens, cracks are observed along the grain boundaries of the IMC phases as seen by the arrow marks in figure 2. The formation of IMC phases in the interface between Cu and Sn results in overall volume shrinkage which increases the residual stresses at the interfaces and grain boundaries of IMC [4], [6]–[8]. The accumulation of the residual stress during isothermal aging induces the crack which propagates along the brittle IMC interface or grain boundary.

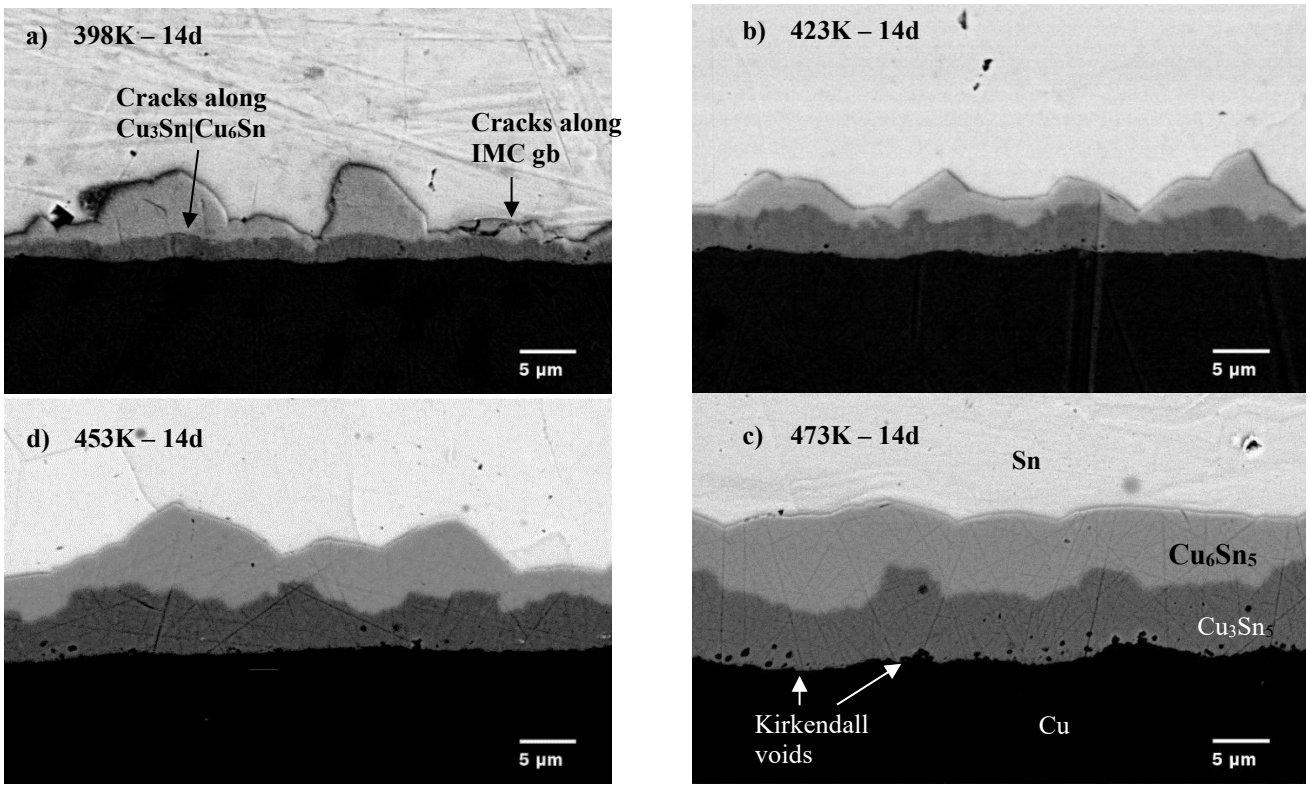

Figure 2: SEM cross section images of rolled Cu – matte Sn diffusion samples aged at a) 398K; b) 423K; c) 453K and d) 473K for 14 days. Cracks are observed along the grain boundaries (gb) of the Cu_6Sn_5 intermetallic (IMC). Kirkendall voids can be observed at the interface between Cu and Cu_3Sn.

These cracks could further develop and lead to early brittle failure of the solder joint. Hence, it is important to control the growth of the IMC phases to reduce the crack formation in the solder joints. The formation and growth of the IMC phases takes place by the interdiffusion of Cu and Sn across the interface. Diffusion of atoms is always accompanied by the diffusion of voids in the opposite direction [9]. The diffusion speed of Cu and Sn is different in different IMC phases [1], [9] (especially at higher temperatures) which lead to formation of Kirkendall voids at the interface between Cu and Cu_3Sn as seen in figure 2. These Kirkendall voids grow and coalesce at longer aging times leading to crack formation between Cu and Cu_3Sn interface [10], [11].

Figure 3 shows the typical EDS composition profile measured across the diffusion zone between Cu and Sn aged at 453K for 14 days. The compositions of the two IMC phases Cu_3Sn and Cu_6Sn_5 were 25.2 at.% Sn and 45.3 at.% Sn. The concentration gradient of Cu_6Sn_5 phase measured by the linear fit of the concentration profile was 2 at.% Sn whereas there was negligible (not detectable by EDS) concentration gradient across Cu_3Sn phase. The terminal phase Cu show negligible solubility of Sn which is in accordance with the Cu-Sn phase diagram[12] . But there was excess Cu concentration of upto 7 at.% Cu (equilibrium Cu concentration in Sn is 0.1 at.% Cu at 453K [12]) detected close to the Cu_6Sn_5|Sn interface as shown by the arrow mark in figure 3. This shows that Cu diffusion is enhanced across the IMC which may be due to the rolled Cu used in this study.

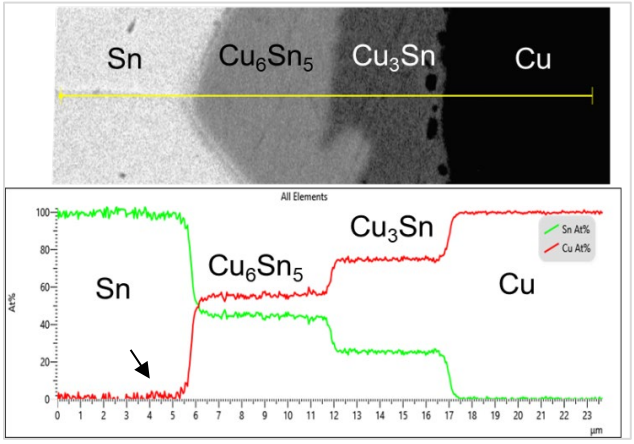

Figure 3: EDS line scan across the Cu-Sn diffusion zone aged at 453K for 14 days.

Growth kinetics of Cu_6Sn_5 and Cu_3Sn IMC phases

The time-dependent growth of the IMC phases (Cu_6Sn_5 and Cu_3Sn) follows growth law according to the equation (1)

$$\ln(x) = n \ln(t) \qquad (1)$$

where x is the thickness of the respective IMC phase for a given aging time t at a particular temperature of interest and n represents the diffusion exponent and can take the value between 0 to 1.

Figure 4 shows the plot between $\ln(x)$ vs $\ln(t)$ where a straight line is fitted to the points at the respective temperatures. The slope of the straight line determines the diffusion exponent n.

The diffusion exponent n from the ln-ln plot (figure 4) shows the probable diffusion mechanism by which growth of the IMC phases take place. When the n value lies between $0< n <0.25$, diffusion is driven by atoms diffusing along the grain boundaries [13]. This is a typical growth mechanism at lower temperatures for most IMC forming systems where it is difficult for the atom to diffuse across the bulk grain and easier along the disordered grain boundaries. At slightly higher temperatures, a mixed mode of diffusion takes place both in the bulk grain as well as along the grain boundaries. As grain growth occurs, the grain boundary area decreases restricting the diffusion of atoms. At these intermediate temperatures, energy is still not high enough for bulk dominant diffusion which reduces the growth rate below the expected parabolic kinetics (n = 0.5). This results in the diffusion exponent to lie between $0.25 < n <0.5$. As the n value increases from 0.25 towards 0.5, the growth mechanism is shifting from grain boundary dominated growth (n = 0.25) towards bulk grain dominated growth (n = 0.5) [13].

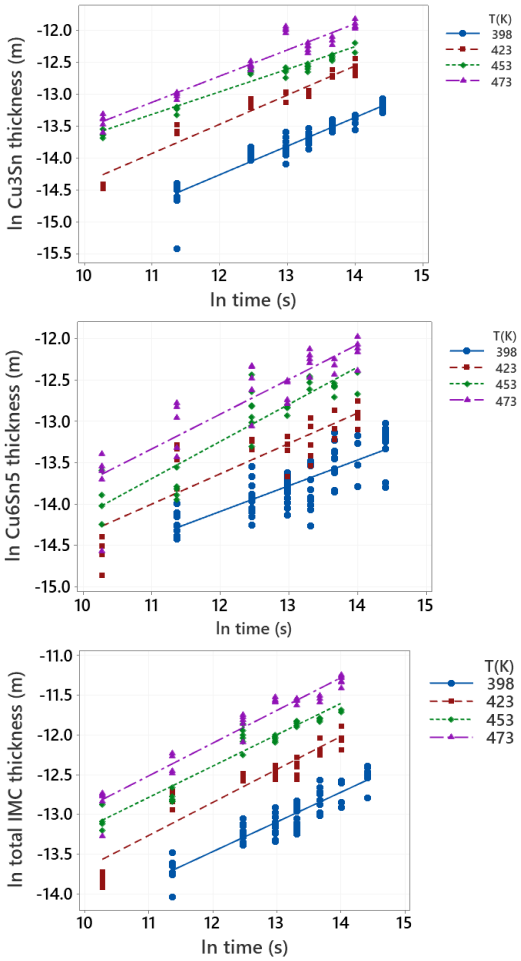

Figure 4: $\ln(x)$ vs $\ln(t)$ plots for Cu_3Sn, Cu_6Sn_5 and the total IMC. The slope determines the diffusion exponent n. The points represent mean IMC thickness of individual SEM images.

Table 2 shows the diffusion exponent n and the goodness-of-fit for figure 4 determined by the R^2 value for Cu_3Sn, Cu_6Sn_5 and the total IMC. R^2 value of 1 corresponds to the perfect

fit. The deviation from perfect fit as seen in table 2 is due to the non-planar morphology of the IMC phases. The value of the diffusion exponent *n* lies between 0.3 – 0.45 in all the cases. This suggests that both Cu_3Sn and Cu_6Sn_5 are in the mixed regime with both grain boundary diffusion and bulk diffusion. In case of Cu_3Sn, the layered growth nature of the IMC is dominated by bulk diffusion in the temperature range between 398K – 473K with a *n* value close to 0.5. For Cu_6Sn_5 phase, the grain boundary diffusion growth is predominant at 398K with a *n* value of 0.3. As temperature increases, bulk diffusion is enabled as shown by the *n* value increase towards 0.5. The Cu_6Sn_5 phase undergoes transition from an ordered crystal structure to a disordered crystal structure upon heating between 445-463K [14]. Hence, at lower temperatures (398K and 423K) where the atoms are ordered in Cu_6Sn_5 crystal, it is easier to diffuse along the grain boundaries. But as temperature increases to 453K or higher, the formation of disordered Cu_6Sn_5 and the increase in concentration of equilibrium point defects in the Cu_6Sn_5 crystal aids in bulk diffusion growth of Cu_6Sn_5 phase.

The competing growth between Cu_3Sn and Cu_6Sn_5 can be evaluated by analyzing the ratio of thickness of Cu_6Sn_5 to that of the total IMC thickness as shown in figure 5. The Cu_6Sn_5 ratio is higher initially (> 0.7) and moves towards 0.5 as time increases at both 398K and 423K. Thermodynamically, the Cu_6Sn_5 has slightly lower Gibbs energy than Cu_3Sn [3]. Hence, Cu_6Sn_5 is the preferred phase to grow initially at lower temperatures and hence results in higher ratios. As time increases, the Cu_3Sn phase grows and the Cu_6Sn_5 ratio decreases with time. At 453K, the Cu_6Sn_5 ratio is small and increases to around 0.5 as time increases and at 473K, the ratio is maintained around 0.45. As temperature is increased, the Cu_3Sn becomes more stable, and it can grow even at lower times. This results in lower Cu_6Sn_5 ratio at higher temperatures. As time increases, the ratio moves towards 0.5 where almost equal thickness of the two IMC phases exists.

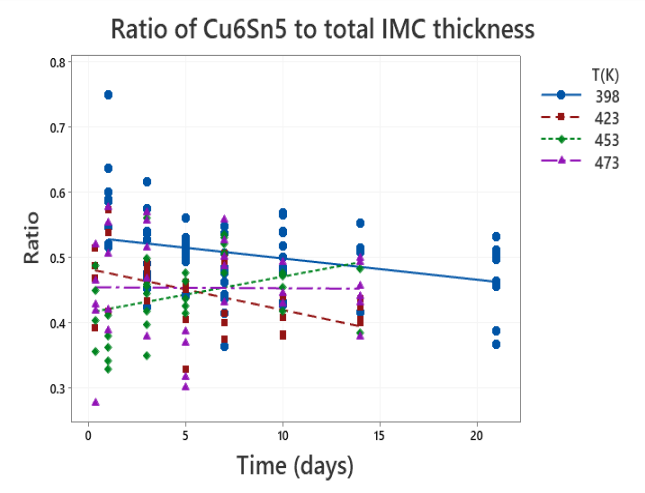

Figure 5: Ratio of Cu_6Sn_5 to the total IMC thickness for different temperatures.

Table 2: Diffusion exponent *n* obtained from the straight line fit from figure 4. SD is the standard deviation for the diffusion exponent *n*. Goodness of fit is shown through the R^2 value. (R^2 = 1 is the perfect fit).

Phase	T(K)	n	SD	R^2
Cu_3Sn	398	0.45	0.02	0.89
	423	0.46	0.02	0.94
	453	0.35	0.02	0.93
	473	0.41	0.01	0.92
Cu_6Sn_5	398	0.31	0.03	0.61
	423	0.37	0.04	0.73
	453	0.45	0.04	0.82
	473	0.42	0.04	0.80
Total IMC	398	0.37	0.02	0.85
	423	0.42	0.03	0.88
	453	0.39	0.02	0.92
	473	0.41	0.02	0.94

Integrated Interdiffusion Coefficients

When calculating the diffusion coefficients and activation energy for a particular phase, it should be property of that individual phase. Often, past studies assume a parabolic growth relationship (n = 0.5) for the IMC phases and calculate a parabolic growth constant (k_p) which can be used to calculate the thickness of the IMC phases for particular aging conditions [2], [4], [9], [10], [15]. In material systems like Cu-Sn, where there is interdependent growth of both Cu_3Sn and Cu_6Sn_5, the system does not perfectly follow the parabolic growth of n = 0.5 as can be seen in this study in table 2 (n<0.5). The diffusion parameter should depend on the growth rate of individual IMC phases even under non-parabolic conditions. Thus, the concept of integrated interdiffusion coefficients as proposed by Wagner *et.al* [5] was used in this study to determine the integrated interdiffusion coefficients (D_{int}) of Cu_3Sn and Cu_6Sn_5.

Table 3 provides the average D_{int} values calculated for Cu_3Sn and Cu_6Sn_5 at various temperatures along with their standard deviations. The D_{int} values for both Cu_3Sn and Cu_6Sn_5 are comparable at all temperatures. This indicates that both phases grow at the same rate at the considered temperature range between 398K – 473K. But the standard deviation for Cu_6Sn_5 is higher at lower temperatures and decreases towards higher temperatures. The rough morphology of the Cu_6Sn_5 at lower temperatures of 398K and 423K is responsible for the higher standard deviations. The higher amount of Cu_3Sn is observed especially at lower temperatures for rolled Cu-Sn system. This could be due to the easier nucleation and grain boundary diffusion growth of the Cu_3Sn.

The temperature dependence of the diffusion growth of the individual IMC phases can be described by the Arrhenius equation (2)[16].

$$D_{int} = D_0 \exp\left(\frac{-E_a}{RT}\right) \quad (2)$$

where D_0 is the diffusion constant in m^2/s, E_a is the activation energy in J, R is the gas constant in J/mol.K and T is the temperature in K. The activation energy (E_a) for the growth of Cu_3Sn and Cu_6Sn_5 is determined from the Arrhenius plot as shown in figure 6.

Table 3: Average D_{int} values obtained for Cu_3Sn and Cu_6Sn_5 at various temperatures. Standard deviations are provided in brackets

T (K)	D_{int} Cu_3Sn (m^2/s) $\times 10^{-18}$	D_{int} Cu_6Sn_5 (m^2/s) $\times 10^{-18}$
398	0.137 (0.021)	0.36 (0.045)
423	0.564 (0.016)	0.42 (0.033)
453	0.947 (0.013)	1.06 (0.013)
473	1.710 (0.013)	1.92 (0.018)

The determined values of E_a and D_0 for Cu_3Sn and Cu_6Sn_5 along with the standard deviation can be seen in table 4. The spread in the data seen in figure 6 is due to the non-planar (wavy) nature of the IMC phases. The normal (mean + SD) approximation of the IMC thickness data (as seen in figure 1) limits the applicability of the model to predict only planar IMC interfaces for specific temperature and time. The normality approximation describes only 50% of the IMC morphology (thickness) data especially for lower temperatures where the IMC thickness is not uniform. Information on influence of Sn grain boundaries (where high IMC thicknesses were observed) on the IMC growth rate is lost in this type of diffusion analysis. Better morphology parameters which preserve the entire morphology information of the IMC surface is needed in future, particularly for extending the diffusion model to material systems containing extremely anisotropic IMC morphologies (Plates, needles etc.,).

The activation energy of Cu_6Sn_5 is slightly higher than that of Cu_3Sn but the Cu_6Sn_5 has one order of magnitude higher D_0 than Cu_3Sn. Activation energies of the order of 50 kJ/moles (0.5 eV/atom) obtained for two IMC phases are low compared to the activation energies found in single crystal bulk diffusion studies (90-150 kJ/mole) [9], [17]–[19]. The lower E_a value observed in this study indicates stronger grain boundary diffusion compared to bulk grain diffusion for both Cu_3Sn and Cu_6Sn_5. Compared to the work of Yuan *et.*al [18] and Paul *et.al* [4], which uses bulk recrystallized Cu and Sn phases with larger grains, the presence of fine grains in rolled Cu (this study) resulted in lower IMC thickness especially at higher temperatures. Rolled Cu is used in the electronic lead frames 80% of the time. Further studies on the impact of rolling direction and texture of the Cu surface on the growth of the IMC phases is required to build a comprehensive IMC growth model.

Table 4: Activation Energy (E_a) and diffusion constant (D_0) of Cu_3Sn and Cu_6Sn_5. Error values for E_a are provided in brackets. Goodness of fit is shown by R^2 values.

Phase	E_a (kJ/mole)	D_0 (m^2/s)	R^2 (m^2/s)
Cu_3Sn	50.5 (3.8)	6.78×10^{-13}	0.90
Cu_6Sn_5	57.2 (6.4)	3.98×10^{-12}	0.81

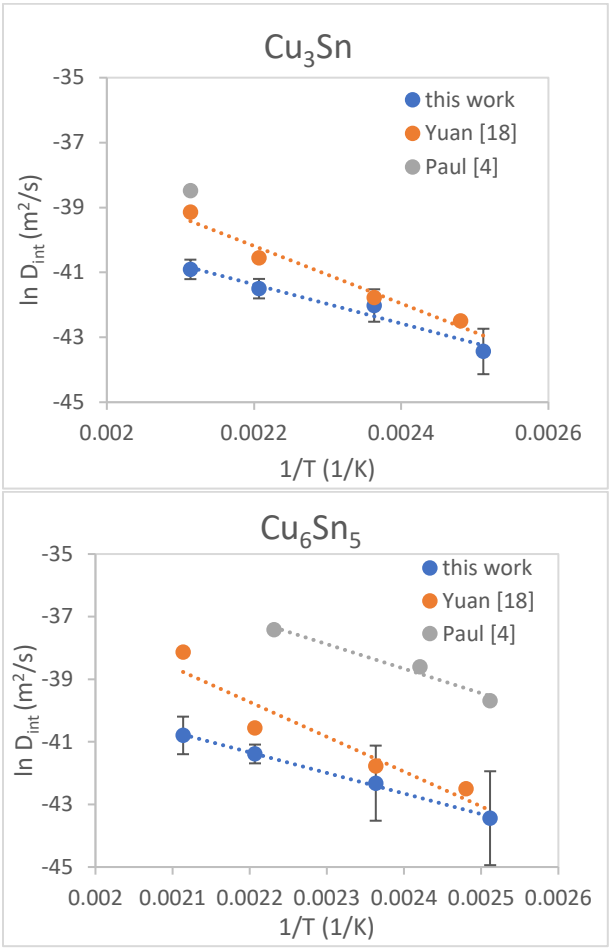

Figure 6: Comparison of D_{int} values of Cu_3Sn and Cu_6Sn_5 obtained in this work with other literature works.

CONCLUSIONS

The following conclusions are obtained from this work regarding the solid-state diffusion in rolled Cu – electroplated Sn system.

- Microstructural investigation revealed the presence of cracks along the grain boundaries of Cu_6Sn_5 and at the interface between $Cu_3Sn|Cu_6Sn_5$ at both low and high temperatures after isothermal aging. This can lead to early failure of the solder joint.

- Integrated interdiffusion coefficients and activation energies for Cu_6Sn_5 and Cu_3Sn have been calculated in this study.
- The lower activation energies of Cu_6Sn_5 and Cu_3Sn confirms grain boundary diffusion growth of IMC phases between 398K – 473K.
- Fine grains in rolled Cu substrate enhances relatively the growth of Cu_3Sn and results in overall lower total IMC thickness at the interface between Cu and Sn.

LIMITATION

The diffusion parameters in this study provide realistic estimates for the average IMC thickness at any temperature between 398K – 473K but caution is advised to extrapolate the calculation to temperatures lower than 398K where the Cu_3Sn phase may be absent depending on the processing conditions.

REFERENCES

[1] S. Kumar, C. A. Handwerker, and M. A. Dayananda, "Intrinsic and Interdiffusion in Cu-Sn System," *J. Phase Equilibria Diffus.*, vol. 32, no. 4, pp. 309–319, Aug. 2011, doi: 10.1007/s11669-011-9907-9.

[2] R. Labie, W. Ruythooren, and J. Van Humbeeck, "Solid state diffusion in Cu–Sn and Ni–Sn diffusion couples with flip-chip scale dimensions," *Intermetallics*, vol. 15, no. 3, pp. 396–403, Mar. 2007, doi: 10.1016/j.intermet.2006.08.003.

[3] M. Onishi and H. Fujibuchi, "Reaction-Diffusion in the Cu–Sn System," *Trans. Jpn. Inst. Met.*, vol. 16, no. 9, pp. 539–547, 1975, doi: 10.2320/matertrans1960.16.539.

[4] A. Paul, C. Ghosh, and W. J. Boettinger, "Diffusion Parameters and Growth Mechanism of Phases in the Cu-Sn System," *Metall. Mater. Trans. A*, vol. 42, no. 4, pp. 952–963, Apr. 2011, doi: 10.1007/s11661-010-0592-9.

[5] C. Wagner, "The evaluation of data obtained with diffusion couples of binary single-phase and multiphase systems," *Acta Metall.*, vol. 17, no. 2, pp. 99–107, Feb. 1969, doi: 10.1016/0001-6160(69)90131-X.

[6] C. Wieser, A. Walnsch, W. Hügel, and A. Leineweber, "The monoclinic lattice distortion of η′-Cu6Sn5," *J. Alloys Compd.*, vol. 794, pp. 491–500, Jul. 2019, doi: 10.1016/j.jallcom.2019.04.265.

[7] G. Kaptay, "Approximated equations for molar volumes of pure solid fcc metals and their liquids from zero Kelvin to above their melting points at standard pressure," *J. Mater. Sci.*, vol. 50, no. 2, pp. 678–687, Jan. 2015, doi: 10.1007/s10853-014-8627-z.

[8] A. Durga, P. Wollants, and N. Moelans, "Phase-field study of IMC growth in Sn–Cu/Cu solder joints including elastoplastic effects," p. 49.

[9] V. A. Baheti, S. Kashyap, P. Kumar, K. Chattopadhyay, and A. Paul, "Solid–state diffusion–controlled growth of the intermediate phases from room temperature to an elevated temperature in the Cu–Sn and the Ni–Sn systems," *J. Alloys Compd.*, vol. 727, pp. 832–840, Dec. 2017, doi: 10.1016/j.jallcom.2017.08.178.

[10] K. Hoshino, Y. Iijima, and K. Hirano, "Interdiffusion and Kirkendall Effect in Cu–Sn Alloys," *Trans. Jpn. Inst. Met.*, vol. 21, no. 10, pp. 674–682, 1980, doi: 10.2320/matertrans1960.21.674.

[11] A. Paul, T. Laurila, V. Vuorinen, and S. V. Divinski, *Thermodynamics, Diffusion and the Kirkendall Effect in Solids*. Cham: Springer International Publishing, 2014. doi: 10.1007/978-3-319-07461-0.

[12] Saunders, N., Miodownik, A.P. The Cu-Sn (Copper-Tin) system. Bulletin of Alloy Phase Diagrams 11, 278–287 (1990). https://doi.org/10.1007/BF03029299

[13] M. Mita, M. Kajihara, N. Kurokawa, and K. Sakamoto, "Growth behavior of Ni3Sn4 layer during reactive diffusion between Ni and Sn at solid-state temperatures," *Mater. Sci. Eng. A*, vol. 403, no. 1–2, pp. 269–275, Aug. 2005, doi: 10.1016/j.msea.2005.05.012.

[14] C. Wieser, W. Hügel, A. Walnsch, and A. Leineweber, "Two-Phase η′ + η Region in Cu6Sn5 Intermetallic: Insight into the Order–Disorder Transition from Diffusion Couples," *J. Electron. Mater.*, vol. 49, no. 1, pp. 245–256, Jan. 2020, doi: 10.1007/s11664-019-07643-3.

[15] S.-W. Chen, S.-H. Wu, and S.-W. Lee, "Interfacial reactions in the Sn-(Cu)/Ni, Sn-(Ni)/Cu, and Sn/(Cu,Ni) systems," *J. Electron. Mater.*, vol. 32, no. 11, pp. 1188–1194, Nov. 2003, doi: 10.1007/s11664-003-0010-9.

[16] Z. Mei, A. J. Sunwoo, and J. W. Morris, "Analysis of low-temperature intermetallic growth in copper-tin diffusion couples," *Metall. Trans. A*, vol. 23, no. 3, pp. 857–864, Mar. 1992, doi: 10.1007/BF02675563.

[17] T. Laurila, V. Vuorinen, and J. K. Kivilahti, "Interfacial reactions between lead-free solders and common base materials," *Mater. Sci. Eng. R Rep.*, vol. 49, no. 1–2, pp. 1–60, Mar. 2005, doi: 10.1016/j.mser.2005.03.001.

[18] K. N. Tu and R. D. Thoimpson, "KINETICS OF INTERFACIAL REACTION IN 3I~ETALLIC Cu-Sn THIN FILMS," p. 6.

[19] Y. Yuan, Y. Guan, D. Li, and N. Moelans, "Investigation of diffusion behavior in Cu–Sn solid state diffusion couples," *J. Alloys Compd.*, vol. 661, pp. 282–293, Mar. 2016, doi: 10.1016/j.jallcom.2015.11.214.